



Thermal analysis of poly(lactic acid) plasticized by cardanol derivatives

Antonio Greco¹ · Francesca Ferrari¹ · Alfonso Maffezzoli¹

Received: 26 October 2017 / Accepted: 7 February 2018
© Akadémiai Kiadó, Budapest, Hungary 2018

Abstract

This work is aimed to study the suitability of cardanol and its derivatives as plasticizers for poly(lactic acid), PLA. Differential scanning calorimetry (DSC) was used to assess the plasticizing effectiveness of cardanol (CARD) and its derivatives, cardanol acetate and epoxidated cardanol acetate, comparing the results with those obtained with a commercially available plasticizer, poly(ethylene glycol), PEG, with an average molecular weight of 400 g mol^{-1} . Measurement of the glass transition temperature highlighted that, among the tested cardanol derivatives, neat cardanol is the most effective plasticizer for PLA. In fact, the glass transition temperature of PLA plasticized by CARD is only slightly higher than that of PLA plasticized by PEG. This is attributed to the lower compatibility between PLA and CARD compared to PLA and PEG, as estimated by the interaction radius. Therefore, cardanol could represent a technically valid, economic, and largely available plasticizer for PLA. Moreover, DSC, an X-ray diffraction analysis, showed that, compared to PEG, the addition of CARD involves a limited increase of the rate of crystallization, even in this case, due to its lower compatibility with PLA. Dynamic mechanical analysis showed that, below glass transition, PEG is able to reduce the stiffness of PLA by a higher extent. However, as the temperature increases, retention of the shear modulus of PEG-plasticized PLA is much higher than that of CARD-plasticized PLA. As a consequence, above glass transition, the stiffness of CARD-plasticized PLA becomes lower than that of PEG-plasticized PLA. Therefore, despite its lower compatibility with PLA, CARD can impart to plasticized PLA lower modulus compared to PEG, when the plasticizer content is high enough to reduce the glass transition below room temperature.

Keywords Poly(lactic acid) · Plasticizer · Cardanol · Glass transition · Crystallization kinetics

Introduction

In recent years, growing environmental awareness has motivated researchers to pay attention to poly(lactic acid) (PLA) for the development of innovative products from bio-based and biodegradable materials. PLA, produced from renewable resources, environmentally and ecologically safe [1], is a good candidate for the replacement of petroleum-based plastics. Due to its high stiffness and strength, similar to those of polystyrene, at least at room temperature, PLA finds application in different industrial fields, such as packaging [2] biocomposites production [3], and can be processed by different techniques, including

extrusion, injection molding [4], calendering, thermoforming, and fiber spinning [5, 6]. The main limitations in the use of PLA arise from its low elongation at break and toughness, mainly when is not quenched and is a semicrystalline polymer. However, gas and vapor barrier properties in packaging applications are dramatically improved when a crystalline phase is present. Therefore, several attempts have been carried out in order to improve the ductility of PLA by copolymerization with other monomers, polymer blending, and the use of plasticizer [7]. In particular, though several biodegradable as well as non-biodegradable plasticizers have been tested to lower the glass transition temperature, increase strain to break, and improve processability [8, 9], low molecular weight poly(ethylene glycol) (PEG) [10, 11] and oligomeric lactic acid [12] were found to give the best results in terms of plasticizing effectiveness. On the other hand, bio-plasticizers, derived from natural oils and properly modified to improve the compatibility with PLA, can represent a valid

✉ Antonio Greco
antonio.greco@unisalento.it

¹ Department of Engineering for Innovation, University of Salento, Via per Monteroni, 73100 Lecce, Italy

alternative to PEG. Cardanol is an industrial grade oil obtained by vacuum distillation of “cashew nut shell liquid” (CNSL), which represents nearly 25% of the total nut weight, and its worldwide availability is estimated to be about 300,000 tons per year. In addition, cardanol is a natural resource characterized by low cost and low toxicological impact, and, being a by-product of cashew nut shell industry, does not require the use of primary resources [13]. Cardanol finds use in resins for coating and polymer industries, as well as in the chemical industry for oil and alcohol soluble resins, laminating resins, and rubber compounding, serving as an excellent raw material for the preparation of high-grade insulating varnishes, paints, enamels [14, 15]. Recently, many studies have established the suitability of cardanol derivatives for the plasticization of poly(vinyl chloride), PVC [16]. Cardanol derivatives showed very promising properties as PVC plasticizer, mainly due to the very good compatibility and low migration during soft PVC service life [17], as well as to its excellent thermal and UV degradation resistance [18]. In particular, the best plasticizing effectiveness was achieved by epoxidated cardanol acetate (ECA), obtained by a double-step chemical modification of cardanol. The good plasticizing effectiveness of epoxidated cardanol acetate draws the attention of industrial partners, leading to the development of a medium-scale industrial plant, for the production of 1 ton of plasticizer [19]. Another cardanol derivative, namely cardanol acetate (CA), was shown to improve toughness and ductility of PLA, to the same extent of phthalate plasticizer, DEHP [20].

This work is aimed to study the suitability of different cardanol derivatives for the plasticization of PLA. Cardanol, cardanol acetate, and epoxidated cardanol acetate were tested at different concentrations, ranging from 10 to 30%. For comparison purposes, poly(ethylene glycol), PEG, was also used. Differential scanning calorimetry (DSC) was used to study the evolution of the glass transition temperature and the crystallization kinetic of the plasticized PLA. XRD analysis was used to estimate the crystalline fraction of the blends produced. Finally, dynamic mechanical analysis (DMA) was carried out in order to measure the evolution of the shear modulus of plasticized PLA as a function of temperature.

Materials and methods

PLA used in this work is the polyester Ingeo Biopolymer 2003D, supplied by NatureWorks (Minnetonka, MN US), characterized by a density of 1.24 g cm^{-3} and a melt flow rate of $6 \text{ g}/600 \text{ s}$ at $210 \text{ }^\circ\text{C}$. According to the producer's technical data sheet, the polymer is mainly composed of L-isomer, with the D-isomer content lower than 4%. PEG,

characterized by a molecular weight $\text{MW} = 400 \text{ g mol}^{-1}$, was purchased from Sigma-Aldrich (St. Louis, MO, US). Technical cardanol, characterized by a purity of 95%, was purchased by Oltremare (Bologna, Italy).

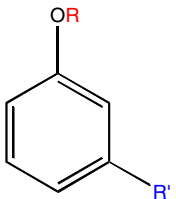
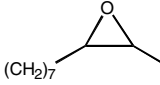
A batch esterification process, involving the conversion of the cardanol hydroxyl group to an acetate group, was performed by mixing 1 mol of cardanol (304.00 g) with 1.5 mol of acetic anhydride (153.13 g), using 0.015 mol (5.58 g) of hexahydrate zinc perchlorate as a catalyst. No solvent was used during the reaction [21, 22]. The mixture was stirred for 24 h at room temperature, after which the cardanol acetate (CA) was washed with distilled water to eliminate the traces of hexahydrate zinc perchlorate. Epoxidized cardanol acetate (ECA) was provided by Serichim (Torviscosa, Udine, Italy) and was obtained by acetylation and further epoxidation of cardanol [17]. The material is characterized by a yield of epoxidation of about 81% with an average molecular weight of about 370 g mol^{-1} . The chemical structures of cardanol and its derivatives are reported in Scheme 1.

Plasticized PLA was obtained by melt mixing of PLA and different amounts of plasticizers (10, 20, and 30% by weight) for 15 min at $190 \text{ }^\circ\text{C}$ in a HAAKE RHEOMIX 600\610 mixer, with a rotor speed of 60 rpm. After mixing, $3 \text{ mm} \times 10 \text{ mm}$ cross section samples were obtained by injection molding through a RayRan hydraulic press, with a barrel temperature of $190 \text{ }^\circ\text{C}$ and a tool temperature of $40 \text{ }^\circ\text{C}$. The thermal treatment on PLA involved some degradation effects, as highlighted by the increase of the intrinsic viscosity (measured by Ubbelohde viscometer according to ASTM D 4603 – 03, by using chloroform as solvent) from 0.15 to 0.44 dL g^{-1} . However, the relatively high temperature of mixing was required in order to obtain efficient plasticization of PLA; in addition, neat PLA was also processed according to the same protocol, in order to account for the change in the thermal properties due to polymer degradation.

DSC analysis was performed on a Mettler Toledo 822 (Mettler Toledo, Greifensee, Switzerland) instrument under a nitrogen flux of 60 mL min^{-1} , applying a first heating scan between -20 and $200 \text{ }^\circ\text{C}$ at $20 \text{ }^\circ\text{C min}^{-1}$, followed by a cooling scan from 200 to $-20 \text{ }^\circ\text{C}$ at $2 \text{ }^\circ\text{C min}^{-1}$ and a second heating scan up to $200 \text{ }^\circ\text{C}$ at $20 \text{ }^\circ\text{C min}^{-1}$.

XRD analysis (Rigaku, Tokyo, Japan) was carried out with $\text{CuK}\alpha$ radiation ($\lambda = 1.5418 \text{ \AA}$) in the step scanning mode recorded in the 2θ range of 10° – 40° , with a step size of 0.02° and step duration of 0.5 s. Finally, dynamic mechanical analysis (DMA) was performed on plasticized PLA samples by using a strain-controlled Rheometrics Ares rheometer, with a torsion geometry, by increasing the temperature from -30 to $60 \text{ }^\circ\text{C}$ at $2 \text{ }^\circ\text{C min}^{-1}$.

Scheme 1 Chemical structures of cardanol and derivatives

		R	R'
	Cardanol	H	C ₁₅ H ₂₅₋₃₁
	Cardanol Acetate (CA)	COCH ₃	C ₁₅ H ₂₅₋₃₁
	Epoxydized Cardanol Acetate (ECA)	COCH ₃	

Results and discussion

The compatibility between PLA and the different plasticizers was initially estimated by calculating the interaction radius. The determination of the interaction radius is based on the Hansen solubility parameter theory and group contribution method, as explained in [21, 23]. The Hansen solubility parameter of PLA and plasticizer can be obtained as the sum of three contributions:

$$\delta^2 = \delta_d^2 + \delta_p^2 + \delta_h^2 \quad (1)$$

where δ_d is the contribution of dispersion forces, δ_p is the contribution of permanent dipoles, and δ_h is the contribution of hydrogen bonding. By introducing a combination of dispersion and polar forces:

$$\delta_v^2 = \delta_d^2 + \delta_p^2 \quad (2)$$

The interaction radius can be obtained as:

$$IR^2 = (\delta_{v,PLA} - \delta_{v,plast})^2 + (\delta_{h,PLA} - \delta_{h,plast})^2 \quad (3)$$

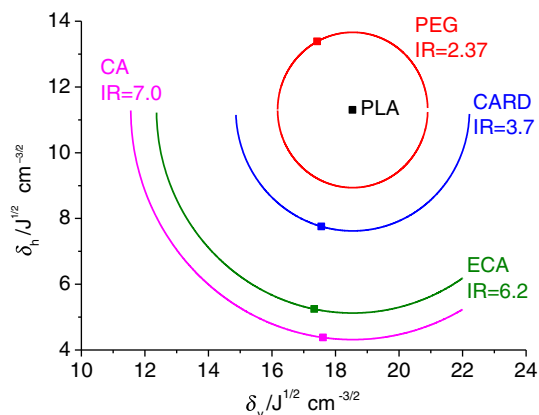
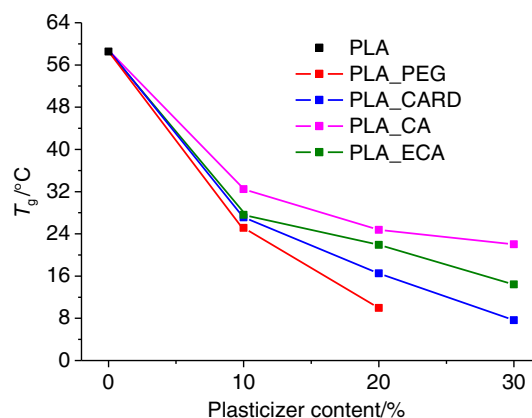
The values of different terms contributing to the Hansen solubility parameters were calculated according to the group contribution method and additivity rule [23]. According to the Hansen solubility parameter theory, a lower interaction radius is indicative of a better

compatibility between the plasticizer and the polymer. The results of Fig. 1 suggest that PEG is, among the tested plasticizers, the one characterized by best compatibility with PLA. Ranking the plasticizers from the higher compatibility to the worst compatibility, PEG > CARD > ECA > CA.

In general, plasticization involves a decrease of the glass transition temperature (T_g) of the polymer, which was measured by DSC during a cooling scan at 2 °C min⁻¹. The results reported in Fig. 2 show a reduction of the glass transition of plasticized PLA compared to that of neat PLA. The glass transition temperature decreases with increasing amount of plasticizer. The missing value for PLA_PEG at 30% plasticizer is due to the absence of the glass transition signal for this sample, due to an almost complete crystallization during cooling in DSC.

The decrease of T_g is dependent on the compatibility between PLA and plasticizer, as evidenced by the results reported in Fig. 3. For each amount of plasticizer, a lower IR, which is indicative of a better compatibility, involves a higher reduction of T_g . Therefore, in accordance with the IR estimation, PEG shows the best plasticizing effectiveness, followed by CARD, ECA, and CA.

Besides the reduction of the glass transition temperature, the addition of the plasticizer also involves a significant

**Fig. 1** δ_v - δ_h diagram for PEG and the tested plasticizer**Fig. 2** Glass transition temperature of plasticized PLA at different plasticizer amounts

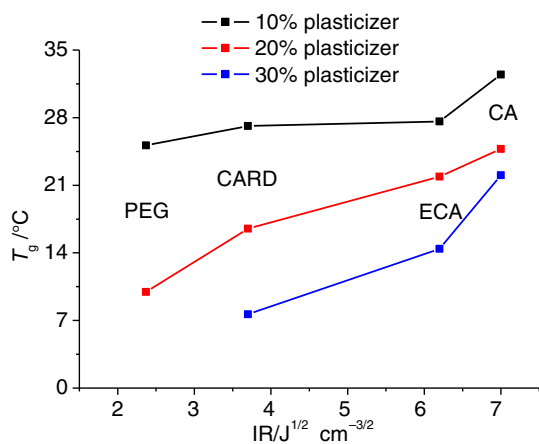


Fig. 3 Evolution of the glass transition temperature as a function of the interaction radius

increase of the crystallization rate [24, 25], as shown by the DSC curves during cooling at 2 °C min^{-1} , reported in Fig. 4a, b. In Fig. 4a, no peak is observed for neat PLA, which indicates that the polymer is not able to crystallize even at the very low cooling rate adopted. Addition of 10% of PEG involves a significant increase of the crystallization kinetics, as evidenced by the large exothermic peak shown in Fig. 4a. This is attributed to the efficient absorption of the plasticizer inside polymer molecules, which increases the free volume and enhances molecular mobility, thus allowing for a faster crystallization [24]. The cardanol-derived plasticizers, CARD and ECA, which are characterized by a reduced compatibility with PLA, show crystallization peaks of decreasing intensity and shifted at lower temperatures. For the less effective plasticizer, CA, the crystallization peak vanishes, indicating that a completely amorphous material is obtained even for very low cooling rates. The effect of the addition of different amounts of plasticizer on crystallization kinetic can be understood by looking at the results reported in Fig. 4b, where the DSC curves for PEG-plasticized PLA are

reported at different amounts of plasticizer. As clearly observed, the crystallization peak shifts to higher temperatures and increases in intensity as the amount of plasticizer is increased, confirming the enhanced molecular mobility brought by the addition of PEG, which results in faster crystallization kinetics.

The different behavior of plasticized PLA during cooling is also reflected in a different behavior during the subsequent heating scan at 20 °C min^{-1} . The results reported in Fig. 5 show, for neat PLA, a clear glass transition signal, which is indicative of the presence of a completely amorphous structure attained during the previous cooling scan. The glass transition signal is overlapped with a significant enthalpy recovery peak, which indicates the presence of structural relaxation of the polymer below T_g [26]. At higher temperature, a weak melting peak results from the presence of some cold crystallization, which occurs very slowly, being not observable on the y-axis scale of Fig. 5. In contrast to neat PLA, a glass transition signal cannot be detected for PLA_PEG, due to the almost completely crystalline structure attained during cooling. At higher temperatures, two broad and intense melting peaks, resulting from the melt crystallization, are observed. This double melting peak indicates the presence of significant recrystallization and lamellar thickening [27]. This is a consequence of the relatively low temperature of melt crystallization, about 80 °C as reported in Fig. 4a, b, which, according to the Hoffman–Weeks equation, involves the formation of quite thin lamellar stacks [28]. DSC heating scans on PLA plasticized by cardanol derivatives show the presence of the glass transition signal, weaker than that observed for neat PLA as a consequence of the presence of a crystalline phase formed during cooling of plasticized PLA, as reported in Fig. 4a. At higher temperatures, a strong exothermic peak is observed, indicating that, compared to neat PLA, the increased free volume and enhanced mobility of the molecules promote cold crystallization. Comparison between the results of

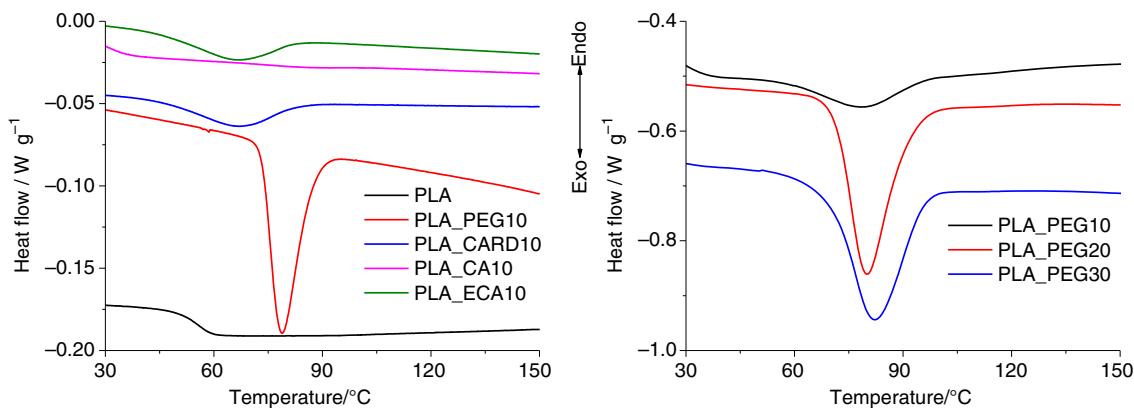


Fig. 4 DSC cooling curves of plasticized PLA: **a** samples with 10% of different plasticizers, **b** samples with a different amount of PEG

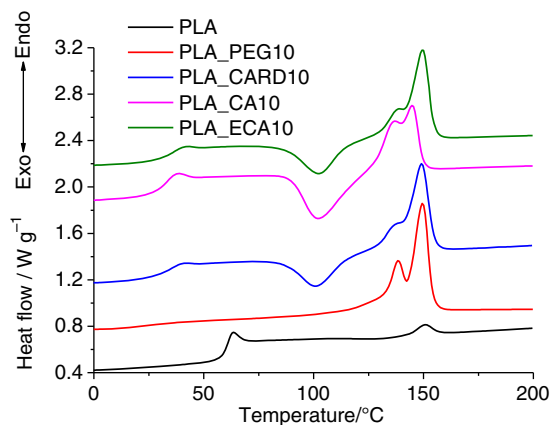


Fig. 5 DSC heating curves of plasticized PLA

Figs. 4 and 5 shows that cold crystallization occurs at higher temperatures than melt crystallization, so involving the formation of thicker crystals. As a consequence, the melting peak of PLA plasticized by cardanol derivatives is characterized by a main melting peak preceded by a shoulder, which reflects the presence of a melt crystallization, occurring at lower temperature, and yielding thinner, lower melting crystals, and a cold crystallization, occurring at higher temperatures, and yielding thicker, higher melting crystals. The same qualitative behavior reported in Fig. 5 was observed for higher amounts of plasticizer (20 and 30%). However, with increasing amount of plasticizer, the glass transition signal becomes weaker, due to the higher crystallinity attained during cooling. For the same reason, the cold crystallization peak is reduced in intensity. In addition, due to enhanced molecular mobility, the cold crystallization peak is shifted to lower temperatures, yielding thinner crystals, which are responsible for a lower onset of melting.

The effect of the enhanced crystallization kinetic brought by the addition of 20% w/w of plasticizer on the structure of plasticized PLA obtained by injection molding was investigated by X-ray diffraction analysis. The results reported in Fig. 6 clearly evidence the amorphous structure of neat PLA. Upon addition of PEG, the presence of a significant crystalline phase is evidenced by the peak at $2\theta = 16.8^\circ$. The intensity of the peak is maximum for PLA_PEG and reduces going to PLA_CARD, finally vanishing for PLA_ECA and PLA_CA. As previously discussed for DSC analysis, the same qualitative behavior is observed for PLA at 10 and 30% of plasticizers. The main difference is related to the higher crystallinity attained during cooling for samples characterized by a higher amount of plasticizer. Therefore, the XRD diffraction peak was found to increase with increasing amount of plasticizer, except for CA and ECA, which show a completely amorphous structure for any amount of plasticizer.

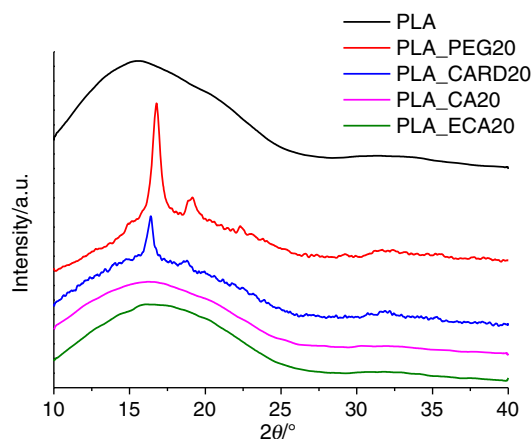


Fig. 6 X-ray diffraction patterns of plasticized PLA

Very interestingly, the crystalline fraction estimated by XRD and by DSC crystallization enthalpy are strongly correlated to the compatibility between plasticizer and PLA. In particular, as shown in Fig. 7, the crystalline phase increases with decreasing interaction radius, which indicates that a better compatibility with the plasticizer causes a faster crystallization during processing. For samples PLA_ECA and PLA_CA, a completely amorphous structure was estimated by XRD analysis, but some melt crystallization enthalpy is obtained in DSC cooling scan, due to the much lower cooling rates of the latter compared to injection molding used for the production of XRD samples. Qualitatively, samples prepared at 10 and 30% plasticizer show the same qualitative behavior, the main difference being related to the increase of melt crystallization enthalpy and XRD degree of crystallinity at higher amounts of plasticizer.

As a result of the change of T_g and crystallization kinetic due to the addition of plasticizer, the evolution of the storage shear modulus in DMA analysis, reported in Fig. 8,

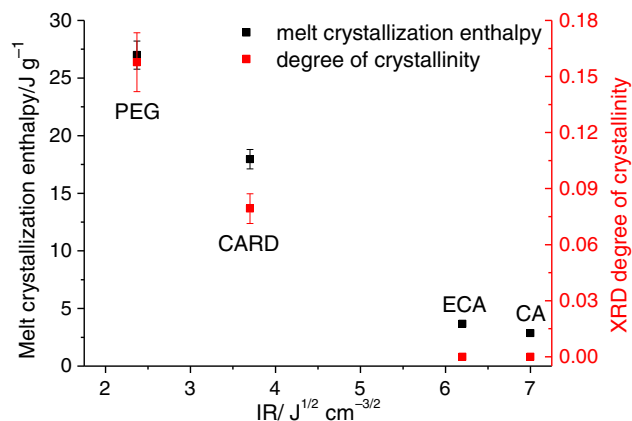


Fig. 7 Melt crystallization enthalpy and crystalline fraction of plasticized PLA as a function of the interaction radius at 20% plasticizer

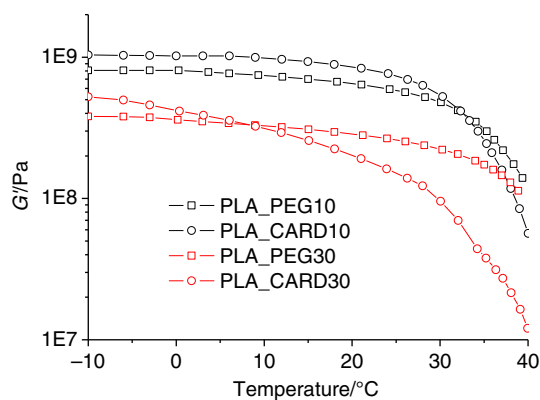


Fig. 8 Storage modulus of plasticized PLA

is significantly influenced by the type and the amount of plasticizer. Referring to the curves at 10% plasticizer, the results of Fig. 8 show that, at low temperatures, G' is higher for PLA_ECA, compared to PLA_PEG. This is in agreement with the basic principles of plasticization, also accounting for the discussed better compatibility of PEG compared to ECA. On the other hand, with increasing temperature, the slope of the curve for PLA_ECA is much higher than that of PLA_PEG. This can be attributed to the higher degree of crystallinity of PLA_PEG, which causes a better retention of the shear modulus as temperature increases. As a consequence of the different slopes, the two curves intersect at a temperature of about 33 °C. Therefore, at room temperature, in the range between 20 and 30 °C, the shear modulus of PEG-plasticized PLA is lower than that of CARD-plasticized PLA, which is in good agreement with the theory of plasticization. As expected, an increase of the amount of plasticizer involves a reduction of the storage modulus. Also at 30% of plasticizer, PLA_PEG shows a better retention of the shear modulus, which again causes intersection of the two curves, but at a much lower temperature, about 10 °C in Fig. 8. Therefore, at room temperature, the shear modulus of PLA_PEG is higher than that of PLA_CARD, thanks to its highly crystalline structure, not modified by the plasticizer which is only absorbed in the amorphous phase. At high plasticizer content, a lower modulus is obtained using a less effective plasticizer, which, despite causing a lower reduction of the glass transition temperature, also reduces the crystallization kinetics and the resulting crystallinity fraction compared to PLA modified with a more effective plasticizer (i.e., PEG).

Conclusions

In this work, the suitability of cardanol and its derivatives as plasticizers for PLA was studied by thermal analysis. The obtained results indicate that, within the composition

limits examined, the addition of cardanol-derived plasticizers involves a reduction of the glass transition temperature, which indicates their good plasticizing effectiveness. In particular, cardanol can produce a reduction of the glass transition temperature of PLA comparable to that observed for PEG. This suggests that cardanol can be used without any chemical modification as PLA plasticizer, as required for the production of cardanol base PVC plasticizers. Furthermore, compared to PEG, the addition of CARD involves a limited increase of the rate of crystallization in comparison with what observed when PEG was used. The effects of plasticizers on the glass transition temperature and crystallization kinetics have been explained using the interaction radius theory. In general, it was possible to assess that a higher plasticizer solubility in PLA involves not only a reduction of the glass transition temperature, but also an increase of the rate of crystallization, both resulting from the increased free volume and enhanced molecular mobility. The two factors have counteracting effects on the evolution of the shear modulus of plasticized PLA:

- At low plasticizer content, the reduction of the glass transition temperature is more relevant than the increase of the rate of crystallization, leading room temperature, still below T_g , or in the T_g range, to lower stiffness when using more compatible plasticizer.
- At higher plasticizer content, the increase of the rate of crystallization becomes more relevant, and therefore a lower modulus is obtained for the less efficient plasticizer at room temperature, which is in this case below T_g .

Therefore, in this case, the lower modulus of cardanol-plasticized PLA can be essentially attributed to a less efficient absorption inside polymer molecules, which reduces the mobility compared to PEG. This poses a relevant issue, related to the leaching and migration of the plasticizer during the service life of plasticized PLA, which determines its durability. This issue, together with a deeper analysis of the mechanical properties of the cardanol-plasticized PLA, will be explored in a future paper.

References

1. Pantani R, De Santis F, Sorrentino A, De Maio F, Titomanlio G. Crystallization kinetics of virgin and processed poly(lactic acid). *Polym Degrad Stab.* 2010;95(7):1148–59.
2. Martino VP, Ruseckaite RA, Jiménez A. Thermal and mechanical characterization of plasticized poly (L-lactide-co-D, L-lactide) films for food packaging. *J Therm Anal Calorim.* 2006;86:707–12.
3. Greco A, Gennaro R, Timo A, Bonfantini F, Maffezzoli A. A comparative study between bio-composites obtained with opuntia

- ficus indica cladodes and flax fibers. *J Polym Environ*. 2013;21(4):910–6.
4. Tábi T, Suplicz A, Czigány T, Kovács JG. Thermal and mechanical analysis of injection moulded poly(lactic acid) filled with poly(ethylene glycol) and talc. *J Therm Anal Calorim*. 2014;118:1419–30.
 5. Lim LT, Auras R, Rubino M. Processing technologies for poly(lactic acid). *Prog Polym Sci*. 2008;33:820–52.
 6. Jamshidian M, Tehrani EA, Imran M, Jacquot M, Desobry S. Poly-Lactic Acid: production, applications, nanocomposites, and release studies. *Compr Rev Food Sci F*. 2010;9(5):552–71.
 7. Ge H, Yang F, Hao Y, Wu G, Zhang H, Dong L. Thermal, mechanical, and rheological properties of plasticized poly(L-lactic acid). *J Appl Polym Sci*. 2013;127(4):2832–9.
 8. Rasal RM, Janorkarc AV, Hirt DE. Poly(lactic acid) modifications. *Prog Polym Sci*. 2010;35:338–56.
 9. Hsieh YT, Kuo NT, Woo EM. Thermal analysis on phase behavior of poly(l-lactic acid) interacting with aliphatic polyesters. *J Therm Anal Calorim*. 2012;107:745–56.
 10. Vieira MG, Altenhofen da Silva M, Oliveira dos Santos L, Beppu M. Natural-based plasticizers and biopolymer films: a review. *Eur Polym J*. 2011;47:254–63.
 11. Martin O, Averous L. Poly(lactic acid): plasticization and properties of biodegradable multiphase systems. *Polymer*. 2001;42:6209–19.
 12. Burgos N, Martino VP, Jiménez A. Characterization and ageing study of poly(lactic acid) films plasticized with oligomeric lactic acid. *Polym Degrad Stab*. 2013;98(2):651–8.
 13. Ionescu M, Wan X, Bilic N, Petrovic ZS. Polyols and rigid polyurethane foams from cashew nut shell liquid. *J Polym Environ*. 2012;20:647–58.
 14. Sakulsaknimitr W, Wirasate S, Pipatpanyanugoon K, Atorngit-jawat P. Structure and thermal properties of polyurethanes synthesized from cardanol diol. *J Polym Environ*. 2015;23:216–26.
 15. Besteti MD, Souza FG Jr, Freire DMG, Pinto JC. Production of core-shell polymer particles-containing cardanol by semibatch combined suspension/emulsion polymerization. *Polym Eng Sci*. 2014;54(5):1222–9.
 16. Greco A, Ferrari F, Del Sole R, Maffezzoli A. Use of cardanol derivatives as plasticizers for PVC. *J Vinyl Addit Technol*. 2016. <https://doi.org/10.1002/vnl.21585>.
 17. Greco A, Ferrari F, Velardi R, Frigione M, Maffezzoli A. Solubility and durability of cardanol derived plasticizers for soft PVC. *Int Polym Proc*. 2016;31(5):577–86.
 18. Greco A, Ferrari F, Maffezzoli A. Ultraviolet and thermal stability of soft poly(vinylchloride) plasticized with cardanol derivatives. *J Clean Prod*. 2017;164:757–64.
 19. Greco A, Ferrari F, Maffezzoli A, Delogu P, Velardi R, Timo A, Tarzia A, Marseglia A, Calò M. Solubility and durability of cardanol derived plasticizers for soft PVC. *Environ Eng Manag J*. 2016;15(9):1989–95.
 20. Greco A, Maffezzoli A. Cardanol derivatives as innovative bioplasticizers for poly-(lactic acid). *Polym Degrad Stab*. 2016;132:213–9.
 21. Greco A, Brunetti D, Renna G, Mele G, Maffezzoli A. Plasticizer for poly(vinyl chloride) from cardanol as a renewable resource material. *Polym Degrad Stab*. 2010;95(11):2169–74.
 22. Calò E, Greco A, Maffezzoli A. Effects of diffusion of a natural derived plasticizer from soft PVC. *Polym Degrad Stab*. 2011;96(5):784–9.
 23. Van Krevelen DW, Te Nijenhuis K. *Properties of Polymers*. 4th ed. Amsterdam: Elsevier; 2009.
 24. Greco A, Maffezzoli A. Analysis of the suitability of polylactic acid in rotational molding. *Adv Polym Technol*. 2015;34(3):21505. <https://doi.org/10.1002/adv.21505>.
 25. Saad GR, Elsayw MA, Aziz MSA. Nonisothermal crystallization behavior and molecular dynamics of poly(lactic acid) plasticized with jojoba oil. *J Therm Anal Calorim*. 2017;128:211–23.
 26. Greco A, Gennaro R, Rizzo M. Glass transition and cooperative rearranging regions in amorphous thermoplastic nanocomposites. *Polym Int*. 2012;61:1326–33.
 27. Pérez-Fonseca AA, Robledo-Ortíz JR, González-Núñez R, Rodrigue D. Effect of thermal annealing on the mechanical and thermal properties of polylactic acid–cellulosic fiber biocomposites. *J Appl Polym Sci*. 2016;133(31):43750.
 28. Wunderlich B. *Macromolecular physics, crystal melting*, vol. 3. New York: Academic Press; 1980.